

10522 814 N 4183  
NACA TN 4183

TECH LIBRARY KAFB, NM  
0066893

# NATIONAL ADVISORY COMMITTEE FOR AERONAUTICS

TECHNICAL NOTE 4183

INVESTIGATION OF EFFECTS OF DISTRIBUTED SURFACE ROUGHNESS  
ON A TURBULENT BOUNDARY LAYER OVER A BODY  
OF REVOLUTION AT A MACH NUMBER OF 2.01

By John R. Sevier, Jr., and K. R. Czarnecki

Langley Aeronautical Laboratory  
Langley Field, Va.



Washington  
February 1958

ATMDC  
TECHNICAL LIBRARY



1H

NATIONAL ADVISORY COMMITTEE FOR AERONAUTICS

TECHNICAL NOTE 4183

INVESTIGATION OF EFFECTS OF DISTRIBUTED SURFACE ROUGHNESS

ON A TURBULENT BOUNDARY LAYER OVER A BODY

OF REVOLUTION AT A MACH NUMBER OF 2.01

By John R. Sevier, Jr., and K. R. Czarnecki

SUMMARY

An investigation has been made of the effects of distributed surface roughness, consisting of lathe-tool marks, on the skin friction of a turbulent boundary layer over a body of revolution at a Mach number of 2.01. The investigation was made on three ogive-cylinders at zero angle of attack over a surface-roughness range from 23 to 480 microinches root mean square and for a Reynolds number range based on body length from  $4 \times 10^6$  to  $30 \times 10^6$ .

The results indicate that the effects of distributed surface roughness on a turbulent boundary layer at a Mach number of 2.01 are generally similar to those found at a Mach number of 1.61 and at subsonic speeds. That is, for a given roughness height, some critical Reynolds number exists at which the skin friction begins to depart from the classical turbulent skin-friction law because of the form drag of the individual roughness particles. The results further indicate that (in the Reynolds number range of these tests) increasing the Mach number from 1.61 to 2.01 increases the allowable roughness for a turbulent boundary layer by about 40 percent. This increase is in good agreement with that predicted on the basis of a constant ratio of allowable roughness height to laminar-sublayer thickness or to a constant value of the Reynolds number based on allowable roughness height, shearing-stress velocity, and local conditions at the surface.

INTRODUCTION

As maximum airplane and missile speeds increase from subsonic to supersonic and hypersonic regimes, the effects of surface roughness on boundary-layer skin friction and heat transfer become of greater importance. Consequently, an investigation (ref. 1) was made in the Langley 4- by 4-foot supersonic pressure tunnel to study the effects

of uniformly distributed roughness on the skin friction of a turbulent boundary layer over a body of revolution at a Mach number of 1.61. The results of reference 1 indicated that the effects of surface roughness (for a turbulent boundary layer) at supersonic speeds were generally the same as those predicted by subsonic-speed theory. The most extensive experimental data available on this subject were Nikuradse's incompressible-flow data (ref. 2 or 3). A comparison was made of the results of reference 1 with those of reference 3, even though it was recognized that the comparison might not be valid because of certain basic differences between the two tests. In spite of the differences, the comparison indicated that there was little or no effect of Mach number on the critical roughness height (where the effects of roughness first appear in a turbulent boundary layer). This indication was not in agreement with the expectation that the thicker laminar sub-layers at higher Mach numbers would increase this height. The absence of this favorable Mach number effect was ascribed to differences in the types of roughnesses investigated and to the different methods of measuring the average roughness heights of the two tests. An extension of the tests in the 4- by 4-foot supersonic pressure tunnel to higher Mach numbers on the same models thus appeared desirable. The purpose of this investigation was to effect this extension.

The present tests were made on the three ogive-cylinder models of reference 1 which had nominal distributed surface roughness, generated by lathe tools, of 23, 240, and 480 microinches root mean square. The models were identical in shape and had an ogive nose 3 calibers in length and an overall fineness ratio of 12.2. Tests were made at zero angle of attack with natural transition and with transition fixed near the model nose over a Reynolds number range from about  $4 \times 10^6$  to about  $30 \times 10^6$ , based on body length. The resulting skin-friction data are compared with the results obtained at a Mach number of 1.61 and with Nikuradse's low-speed-flow data.

SYMBOLS

- |           |                                     |  |
|-----------|-------------------------------------|--|
| $C_{D,T}$ | total-drag coefficient,             | $\frac{D}{qS_f}$                             |
| $C_{D,b}$ | base drag coefficient,              | $\frac{P_b - P_\infty}{qS_f} S_b$            |
| $C_{D,p}$ | forebody pressure-drag coefficient, | $\frac{\text{Forebody pressure drag}}{qS_f}$ |

|                  |  |
|------------------|--|
| $C_{f,f}$        | skin-friction drag coefficient based on $S_f$ ,<br>$C_{D,T} + C_{D,b} - C_{D,p}$   |
| $C_{f,w}$        | skin-friction drag coefficient based on $S_w$ , $C_{f,f} \frac{S_f}{S_w}$  |
| $\Delta C_{f,w}$ | incremental skin-friction coefficient with turbulent<br>boundary layer, $(C_{f,w})_{\text{rough model}} - (C_{f,w})_{\text{smooth model}}$ |
| $c_f$            | local skin-friction drag coefficient   |
| D                | total drag   |
| d                | model diameter   |
| k                | roughness height, root-mean-square values  |
| $k'$             | roughness height, absolute values, $\frac{1}{0.707} k$   |
| $k'_{ad}$        | admissible or allowable roughness height, absolute values  |
| L                | model length   |
| M                | Mach number  |
| $p_b$            | base pressure  |
| $p_\infty$       | free-stream static pressure  |
| q                | free-stream dynamic pressure   |
| R                | free-stream Reynolds number, based on body length, $\frac{UL}{\nu}$  |
| $R_{ft}$         | Reynolds number per foot   |
| r                | radius of curvature  |
| $S_b$            | base area of model, $S_b = S_f$  |
| $S_f$            | maximum frontal area of model  |
| $S_w$            | total wetted surface area of model   |

|            |                                    |
|------------|------------------------------------|
| T          | temperature                        |
| U          | velocity of free stream            |
| u          | local velocity                     |
| $v_*$      | shearing-stress velocity           |
| y          | distance from model surface        |
| $\gamma$   | ratio of specific heats            |
| $\delta_L$ | laminar-sublayer thickness         |
| $\eta_r$   | temperature-recovery factor        |
| $\mu$      | coefficient of viscosity           |
| $\nu$      | coefficient of kinematic viscosity |
| $\rho$     | density                            |
| $\tau$     | shearing stress                    |

Subscripts:

|   |  |
|---|--|
| o | properties evaluated just outside boundary layer |
| t | stagnation                                       |
| W | properties evaluated at wall                     |

## APPARATUS AND METHODS

### Wind Tunnel and Models

The investigation was made in the Langley 4- by 4-foot supersonic pressure tunnel. Calibration of the test-section flow at  $M = 2.01$  indicates a Mach number variation of about  $\pm 0.01$  and no significant flow irregularities in the stream flow direction.

The aluminum models were bodies of revolution composed of a 3-caliber ogive nose with a 9.2-caliber cylindrical afterbody. (See fig. 1.) Approximately constant, uniformly distributed roughness was

produced by lathe-tool marks on the entire surface of each model (fig. 2), except at the surface near the nose (approximately the first 2 inches) where control of the roughness was impossible. The average roughness, dimensions, and areas of the models are given in the following table:

| L, in. | d, in. | k,<br>μin. rms | S <sub>f</sub> , sq ft | S <sub>w</sub> , sq ft |
|--------|--------|----------------|------------------------|------------------------|
| 50.0   | 4.03   | 23 ± 5         | 0.0886                 | 4.05                   |
| 50.1   | 4.06   | 240 ± 60       | .0899                  | 4.08                   |
| 49.9   | 4.08   | 480 ± 50       | .0908                  | 4.09                   |

The manner in which the roughness was produced and the subsequent rounding off of the peaks resulted in a roughness profile which was approximately a sine wave. Surface roughness of the models was measured in microinches, root mean square, by means of a Physicists Research Co. Profilometer, Model No. 11.

The models were sting mounted. Total-drag measurements were made with a single-component strain-gage balance. Base pressures were determined by taking an average of the values given by four tubes spaced at 90° intervals along the sting in the plane of the base. A 4-inch-long cylindrical wooden block having approximately the same diameter as that of the models was positioned about 1/8 inch behind the model base for tests of the models to reduce the base drag (by increasing the base pressure) and thereby reduce the load on the balance at high stagnation pressures.

#### Tests

All tests were made with the models at zero angle of attack through a stagnation-pressure range from 3 to about 30 lb/sq in. abs, corresponding to Reynolds numbers based on model length of about  $4 \times 10^6$  to  $30 \times 10^6$ . Tunnel stagnation temperatures, depending on the stagnation pressure, varied from about 90° F to 130° F. The tunnel dew-point was sufficiently low to prevent significant condensation effects.

Drag and base-pressure data were taken through the Reynolds number range on all the models with fixed transition and on the 23- and

480-microinch-roughness models with natural transition. Transition was fixed about 1/2 inch behind the nose of the model with No. 60 carborundum grains cemented to the model surface. Considerable difficulty was encountered in obtaining body-drag measurements with natural transition at high Reynolds numbers free of the "sandblasting" effects of particles in the tunnel airstream. The pits and peaks produced by these particles on the soft surface were removed as completely as possible, and runs were repeated with each model in an attempt to obtain data free of sandblasting effects.

In order to obtain forebody pressure drag, pressure distributions were obtained on an 85-microinch-roughness body through the Reynolds number range. For the 480-microinch-roughness model, schlieren observations were also made over a Reynolds number range from about  $6 \times 10^6$  to  $29 \times 10^6$ .

#### Data Reduction

The values of skin-friction drag coefficient were obtained by subtracting the forebody pressure-drag coefficient from the total-drag coefficient (determined by means of the balance) and adjusting the measured base pressure to correspond with free-stream static pressure. The forebody pressure drag was determined from measured pressure distributions over the nose for a Reynolds number range from about  $6 \times 10^6$  to about  $24 \times 10^6$ . Since the variation of the value of  $C_{D,p}$  with Reynolds number was of about the same order as the scatter in the data, a constant value of  $C_{D,p} = 0.085$  was used throughout the Reynolds number range for all the models.

#### Corrections and Accuracy

No corrections were made for buoyancy since this effect was found to be negligible. Previous calibrations have shown a slight decrease in test-section Mach number at stagnation pressures below 4 lb/sq in. abs. However, estimates indicate that no corrections to the data are required.

The maximum error in skin-friction drag coefficient at the higher Reynolds numbers from  $25 \times 10^6$  to  $30 \times 10^6$  is estimated to be about  $\pm 0.0001$  (based on wetted area); in the Reynolds number range from  $10 \times 10^6$  to  $12 \times 10^6$  the maximum error is about  $\pm 0.0002$ ; and at the

lowest Reynolds numbers (about  $4 \times 10^6$ ), the error may be as great as  $\pm 0.0005$ . However, based on the repeatability of the data over two or three runs, it is believed that, for the data presented herein, the values of skin friction (especially in the lower Reynolds number range) are not as inaccurate as are indicated by the maximum errors.

## RESULTS AND DISCUSSION

### General Remarks

As in the investigation at  $M = 1.61$  (ref. 1), considerable difficulty was experienced in obtaining reliable skin-friction data for the natural-transition case because of sandblasting effects on the relatively soft aluminum models. However, since the primary objective of the present investigation was to determine the effects of distributed surface roughness on a turbulent boundary layer at a given Mach number, most of the tests were made with transition fixed near the nose. A limited amount of natural-transition data are presented for the 23- and 480-microinch-roughness models and represent the best data obtained from two or three runs on each model. For fixed transition, the effects of sandblasting do not influence the measurements. Each model was tested at least twice with the reruns checking very closely with the original runs.

In figure 3 are presented typical data, in coefficient form, showing the variation with Reynolds number of total drag (as measured by the internal balance), base drag, and the resulting skin-friction drag. As mentioned previously, the pressure-drag coefficient was measured and found to be 0.085 and was constant over the Reynolds number range. The data presented in figure 3 are the result of two or more runs of a given model; the different levels of base drag coefficient (and, therefore, total-drag coefficient) are a result of the fact that the gap between the model base and the wooden-base plug was not kept absolutely constant from one run to the next.

### Effects of Surface Roughness on Skin Friction

In figure 4 are presented the results of the skin-friction drag coefficient (based on wetted surface area) as a function of Reynolds number (based on body length) for the three roughness heights tested. The theoretical curves were obtained by the extended Frankl-Voishel method (ref. 4) for the turbulent boundary layer and by the Chapman-Rubesin method (ref. 5) for the laminar boundary layer. Mangler's



transformation (ref. 6), with the additional assumption of zero pressure gradient on the model, was used to modify these results and obtain values applicable to the ogive-cylinder body investigated.

Examination of figures 4(a) and 4(c) for the 23- and 480-microinch-roughness models, respectively, indicates that the experimental skin friction (for the natural-transition case) never quite reaches the theoretical laminar level even at the lowest Reynolds number. It is of interest to note that the drag data are least reliable in this low Reynolds number range because the forces measured by the strain-gage balance are only a small percentage of full-scale deflection.

On the basis of experience gained in reference 1, it is believed that the abrupt jumps in skin-friction drag coefficient in the transitional region (figs. 4(a) and 4(c)) are a result of the models becoming sandblasted.

The agreement of the fixed-transition data with the turbulent-boundary-layer theory is considered to be good, particularly for the 23- and 240-microinch-roughness models. A possible explanation for the fact that the skin-friction data for the 480-microinch-roughness model is somewhat higher than theory may be that this roughness is sufficiently great to cause additional wave drag, at least over the forward part of the model where the boundary layer is relatively thin. As mentioned previously, the forebody pressure drag used in the reduction of all the data was that measured on a smoother model (85 microinches root mean square).

Examination of figure 4(c) for the 480-microinch-roughness model shows the expected trend in  $C_{f,w}$  with Reynolds number for the turbulent boundary layer. In the lower Reynolds number range ( $4 \times 10^6$  to  $10 \times 10^6$ ), the skin-friction curve decreases with increasing Reynolds number and extends parallel to the theoretical curve until, at some point, it begins to diverge from the theoretical curve and finally becomes constant (in the range of these tests) as the Reynolds number continues to increase. This behavior was first noted by Nikuradse in low-speed tests of sand-roughened pipes (ref. 2), and the same effect was found at supersonic speeds in reference 1. In the present tests, the divergence Reynolds number was found to be  $11 \times 10^6$  for the 480-microinch-roughness model and  $24 \times 10^6$  for the 240-microinch-roughness model. The divergence Reynolds number for the 23-microinch-roughness model was, as expected, above the Reynolds number range of the present tests.

### Comparison With Results at $M = 1.61$

In reference 1, a comparison was made between the data for the allowable roughness height of the ogive-cylinders at  $M = 1.61$  and the most extensive data available (ref. 3) which were low-speed data on sand-roughened flat plates (which Schlichting had converted from Nikuradse's original experiments in ref. 2 on sand-roughened pipes). The values of allowable roughness for the low-speed data were taken directly from the curves shown in reference 3 rather than by applying the less representative formula indicated by Schlichting. The comparison indicated that the allowable roughness heights for the two tests were in close agreement; however, it was recognized that the agreement may have been fortuitous because of possible errors in measuring the absolute roughness height on the ogive-cylinder model, the different type of roughness used in the investigations (circumferential ridges and sand grains), and the fact that three-dimensional boundary-layer flow occurs on the ogive-cylinder and two-dimensional boundary-layer flow occurs on the flat plate. This agreement between references 1 and 3 is discussed in more detail later in light of the results of the present tests.

Examination of figure 5 indicates a considerable increase in allowable roughness height between  $M = 1.61$  and  $M = 2.01$ , at least in the Reynolds number range of these tests. Since only two data points exist for each Mach number and these points are subject to inaccuracies in determining divergence Reynolds number, it is difficult to determine precisely the magnitude of this increase. However, for any reasonable straight-line fairing (as low-speed results would indicate), there is about a 40-percent increase in allowable roughness from  $M = 1.61$  to  $M = 2.01$ . If this strong Mach number effect on allowable roughness can be expected to hold to higher Mach numbers, then the favorable effect of increasing Mach number at a given altitude overshadows the unfavorable effect of increasing Reynolds number on the allowable roughness (because of thinning the boundary layer) and results in an overall increase in allowable roughness at the higher Mach number. Before such a result can be verified, it will be necessary to extend the present tests to higher Mach numbers and higher Reynolds numbers.

The reason for the large increase in allowable roughness height between  $M = 1.61$  and  $M = 2.01$  can be explained on the basis of the following discussion. In the classical pipe flow work (ref. 2), it was determined that the characteristic parameter involved was the ratio of roughness height to laminar-sublayer thickness. If the roughness height is sufficiently small in comparison to the laminar-sublayer thickness, the effect of roughness on turbulent skin friction is negligible and the skin friction is dependent only upon Reynolds number. On the other hand, if the roughness height is sufficiently large such that all the roughness particles project out of the laminar sublayer, the friction drag becomes predominantly the form drag of the individual

roughness particles. In this range, the friction drag is independent of Reynolds number and depends only upon the relative roughness. An intermediate region exists between these two extremes in which the friction drag depends on both the Reynolds number and the relative roughness. Thus, on the basis of these early pipe experiments, it would be expected that whatever Mach number effect existed between the present tests and those of reference 1 would be a result of the increase in laminar-sublayer thickness and, moreover, that the magnitude of the increase in allowable roughness height would be of the same order as the increase in laminar-sublayer thickness at a given Reynolds number. This reasoning appears to be in good agreement with the results since the increase in laminar-sublayer thickness between  $M = 1.61$  and  $M = 2.01$  was calculated to be about 30 percent (see the appendix), whereas the measured increase in allowable roughness height was about 40 percent. Therefore, within the accuracy of the data, it may be concluded that

the Reynolds number  $\frac{v_* k'_{ad}}{v}$ , based on allowable roughness height,

shearing-stress velocity, and local conditions at the surface, is independent of Mach number, at least in the Mach number range from 1.6 to 2.0. This is equivalent to stating that the ratio of allowable roughness height to laminar-sublayer thickness is independent of Mach number.

An item of interest is the change which occurs in the laminar-sublayer thickness (and, therefore, in the allowable roughness) because of the combined effect of increasing Mach number and Reynolds number. Such a calculation would be of more practical interest than one based on changing Mach number and constant Reynolds number, because a change in Mach number would usually result in a change in Reynolds number. For example, if the present configuration were operating at a constant altitude and the Mach number were increased from 1.61 to 2.01 (see fig. 5), the favorable Mach number effect in combination with the unfavorable Reynolds number effect would result in a net favorable effect of increasing the allowable roughness by 10 to 15 percent, as compared with about a 40-percent increase for the constant Reynolds number case. On the basis of the analysis presented in the appendix, if the Mach number had increased from 1.61 to 5.0 (at constant altitude), the allowable roughness would be increased by a factor of 3.5 as compared with a factor of 10 for the constant Reynolds number case.

A matter to note is that surface cooling, at a given Mach number and Reynolds number, will serve to reduce the laminar-sublayer thickness and thereby reduce the allowable roughness height. On the basis of this analysis, then, the agreement between the allowable roughness heights of the low-speed experiments of reference 3 and those of the investigation of reference 1 at  $M = 1.61$  appears to be merely fortuitous (as was suggested in ref. 1) since a rough calculation indicates a 100-percent change in laminar-sublayer thickness between

the two investigations at the same Reynolds number. Apparently, the previously mentioned differences between the investigations of references 1 and 2 invalidate any sort of direct comparison of allowable roughness heights.

The variation of incremental skin-friction drag coefficient due to adding roughness  $\Delta C_{f,w}$  with Reynolds number and Reynolds number per foot is shown in figure 6 for the 480-microinch-roughness model ( $k' = 0.00068$  inch and  $k'/L = 1.4 \times 10^{-5}$ ). Results of the 240-microinch-roughness model are not included in figure 6 since the divergence Reynolds number is so close to the maximum test Reynolds number that only a small range of data are available. As mentioned previously,  $\Delta C_{f,w}$  for low speeds consists mainly of the form drag of the individual roughness particles which project from the laminar sub-layer. In addition, at supersonic speeds, these roughness particles would be expected to give rise to wave drag. This condition is substantiated by the schlieren photograph of figure 7 in which weak shock waves can be seen emanating from the roughness particles, particularly over the forward part of the body where the laminar sublayer is thinnest. Therefore,  $\Delta C_{f,w}$  would be expected to increase more rapidly with Reynolds number at  $M = 2.01$  than at low speeds. In fact, with an extremely sensitive balance, detection of an increase in  $\Delta C_{f,w}$  between  $M = 1.61$  and  $M = 2.01$  should be possible, provided the base drag is measured with sufficient accuracy. However, a comparison of the present data with the low-speed data (ref. 3) and with the data at  $M = 1.61$  (ref. 1) does not indicate any effects consistent with the previous discussion. Two possible explanations for this result might be that (1) the comparison with low-speed results is not valid because of the previously discussed differences between the low-speed and supersonic tests, and (2) the balance employed in the present tests was not sensitive enough to measure the relatively small wave drag of the roughness particles.

#### CONCLUDING REMARKS

An investigation has been made of the effects of distributed surface roughness, consisting of lathe-tool marks, on the skin friction of a turbulent boundary layer over a body of revolution at a Mach number of 2.01. The tests were made on three ogive-cylinders at zero angle of attack over a surface-roughness range from 23 to 480 micro-inches root mean square and for a Reynolds number range based on body length from  $4 \times 10^6$  to  $30 \times 10^6$ .

The effects of distributed surface roughness on a turbulent boundary layer at a Mach number of 2.01 are found to be generally similar to those at a Mach number of 1.61 and at subsonic speeds. That is, for a given roughness height, some critical Reynolds number exists at which the skin friction begins to depart from the classical turbulent skin-friction law because of the form drag of the individual roughness particles. In the Reynolds number range of these tests, increasing the Mach number from 1.61 to 2.01 increases the allowable roughness for a turbulent boundary layer by about 40 percent. This increase is in good agreement with that predicted on the basis of a constant ratio of allowable roughness height to laminar-sublayer thickness or to a constant value of the Reynolds number based on allowable roughness height, shearing-stress velocity, and local conditions at the surface.

Langley Aeronautical Laboratory,  
National Advisory Committee for Aeronautics,  
Langley Field, Va., September 24, 1957.

APPENDIX

ESTIMATION OF CHANGE IN LAMINAR-SUBLAYER THICKNESS

FROM  $M = 1.61$  TO  $M = 2.01$

On the basis of the universal velocity distribution (fig. 8), it is assumed that the quantity  $\frac{\delta_L v_*}{\nu}$  is independent of Mach number. That is, if

$$\frac{\delta_L v_*}{\nu} = \text{Constant} = C$$

then,

$$\delta_L = \frac{C\nu}{v_*} \tag{1}$$

where the properties are evaluated at the outer edge of the laminar sublayer. Since the temperature at the wall is about the same as that at the outer edge of the laminar sublayer, the properties in equation (1) can be taken to be the wall values with little loss in accuracy.

If the following expressions are substituted into equation (1):

$$v_W = \frac{\mu_W}{\rho_W}$$

$$v_* = \sqrt{\frac{\tau_W}{\rho_W}}$$

then,

$$\begin{aligned} \delta_L &= \frac{C\mu_W}{\sqrt{\tau_W\rho_W}} \\ &= \frac{C \frac{\mu_W}{\mu_0} \mu_0}{\sqrt{\frac{\tau_W}{\rho_0}} \sqrt{\frac{\rho_W}{\rho_0}} \rho_0} \end{aligned}$$

where the subscript  $o$  denotes that the properties are evaluated just outside the turbulent boundary layer.

Since

$$c_f = \frac{\tau_w}{\frac{1}{2} \rho_o U_o^2}$$

and

$$R_{ft,o} = \frac{\rho_o U_o}{\mu_o}$$

then,

$$\delta_L = \frac{C \frac{\mu_w}{\mu_o} \sqrt{\frac{\rho_o}{\rho_w}}}{\sqrt{\frac{1}{2} c_f R_{ft,o}}}$$

The ratio of  $(\delta_L)_{M=2.01}$  to  $(\delta_L)_{M=1.61}$  at the same free-stream Reynolds number is

$$\frac{(\delta_L)_{M=2.01}}{(\delta_L)_{M=1.61}} = \frac{\left( \frac{\mu_w}{\mu_o} \sqrt{\frac{\rho_o}{\rho_w}} \right)_{M=2.01}}{\left( \frac{\mu_w}{\mu_o} \sqrt{\frac{\rho_o}{\rho_w}} \right)_{M=1.61}} \sqrt{\frac{(c_f)_{M=1.61}}{(c_f)_{M=2.01}}}$$

If it is assumed that there is no variation in static pressure across the boundary layer, the perfect-gas law gives

$$\sqrt{\frac{\rho_o}{\rho_w}} = \sqrt{\frac{T_w}{T_o}}$$

For simplicity, a linear variation of viscosity with temperature is assumed. Thus,

$$\frac{\mu_W}{\mu_O} = \frac{T_W}{T_O}$$

For the local skin-friction drag coefficient, the extended Frankl-Voishel expression is used which gives

$$c_f = \frac{0.472}{\left(\log_{10} R_o\right)^{2.58} \left(1 + \frac{\gamma - 1}{2} M^2\right)^{0.467}} \left(1 - \frac{1.12}{\log_{10} R_o}\right)$$

At the same free-stream Reynolds number  $\left((R_o)_{M=1.61} = (R_o)_{M=2.01}\right)$ ,

$$\sqrt{\frac{(c_f)_{M=1.61}}{(c_f)_{M=2.01}}} = \sqrt{\frac{\left(1 + \frac{\gamma - 1}{2} M_{2.01}^2\right)^{0.467}}{\left(1 + \frac{\gamma - 1}{2} M_{1.61}^2\right)^{0.467}}}$$

Then,

$$\frac{(\delta_L)_{M=2.01}}{(\delta_L)_{M=1.61}} = \frac{\left(\frac{T_W}{T_O}\right)_{M=2.01}^{3/2} \left(1 + \frac{\gamma - 1}{2} M_{2.01}^2\right)^{0.2335}}{\left(\frac{T_W}{T_O}\right)_{M=1.61}^{3/2} \left(1 + \frac{\gamma - 1}{2} M_{1.61}^2\right)}$$

Since

$$\eta_r = \frac{T_W - T_O}{T_t - T_O}$$

and

$$\frac{T_t}{T_O} = 1 + \frac{\gamma - 1}{2} M^2$$



then,

$$\frac{T_w}{T_o} = 1 + \eta_r \left( \frac{\gamma - 1}{2} M^2 \right)$$

For a recovery factor  $\eta_r$  of 0.90 with  $\gamma = 1.4$ :

$$\frac{(\delta_L)_{M=2.01}}{(\delta_L)_{M=1.61}} = \frac{(1 + 0.18 M_{2.01}^2)^{3/2} \left( \frac{1 + 0.2 M_{2.01}^2}{1 + 0.2 M_{1.61}^2} \right)^{0.2335}}{(1 + 0.18 M_{1.61}^2)^{3/2}}$$

Substituting the indicated values of  $M$  into the preceding equation gives

$$(\delta_L)_{M=2.01} = 1.331 (\delta_L)_{M=1.61}$$

If the more exact variation of viscosity with temperature as given by Sutherland's formula had been used, the result would have been (in the temperature range of these tests)

$$(\delta_L)_{M=2.01} = 1.313 (\delta_L)_{M=1.61}$$

This estimate for the change in laminar-sublayer thickness with Mach number has been made only for a flat plate and should be modified somewhat to apply over the forward part of the ogive-cylinder where a pressure gradient exists. An estimate was made for the change in laminar-sublayer thickness (from  $M = 1.61$  to  $M = 2.01$ ) over the ogive-cylinder of the present investigation, and a difference of less than 5 percent from the flat-plate result was found to exist.

REFERENCES

1. Czarnecki, K. R., Robinson, Ross B., and Hilton, John H., Jr.: Investigation of Distributed Surface Roughness on a Body of Revolution at a Mach Number of 1.61. NACA TN 3230, 1954.
2. Nikuradse, J.: Laws of Flow in Rough Pipes. NACA TM 1292, 1950.
3. Schlichting, H.: Lecture Series "Boundary Layer Theory." Part II - Turbulent Flows. NACA TM 1218, 1949.
4. Rubesin, Morris W., Maydew, Randall C., and Varga, Steven A.: An Analytical and Experimental Investigation of the Skin Friction of the Turbulent Boundary Layer on a Flat Plate at Supersonic Speeds. NACA TN 2305, 1951.
5. Chapman, Dean R., and Rubesin, Morris W.: Temperature and Velocity Profiles in the Compressible Laminar Boundary Layer With Arbitrary Distribution of Surface Temperature. Jour. Aero. Sci., vol. 16, no. 9, Sept. 1949, pp. 547-565.
6. Mangler, W.: Boundary Layers With Symmetrical Airflow About Bodies of Revolution. Rep. No. R-30-18, pt. 20, Goodyear Aircraft Corp., Mar. 6, 1946.

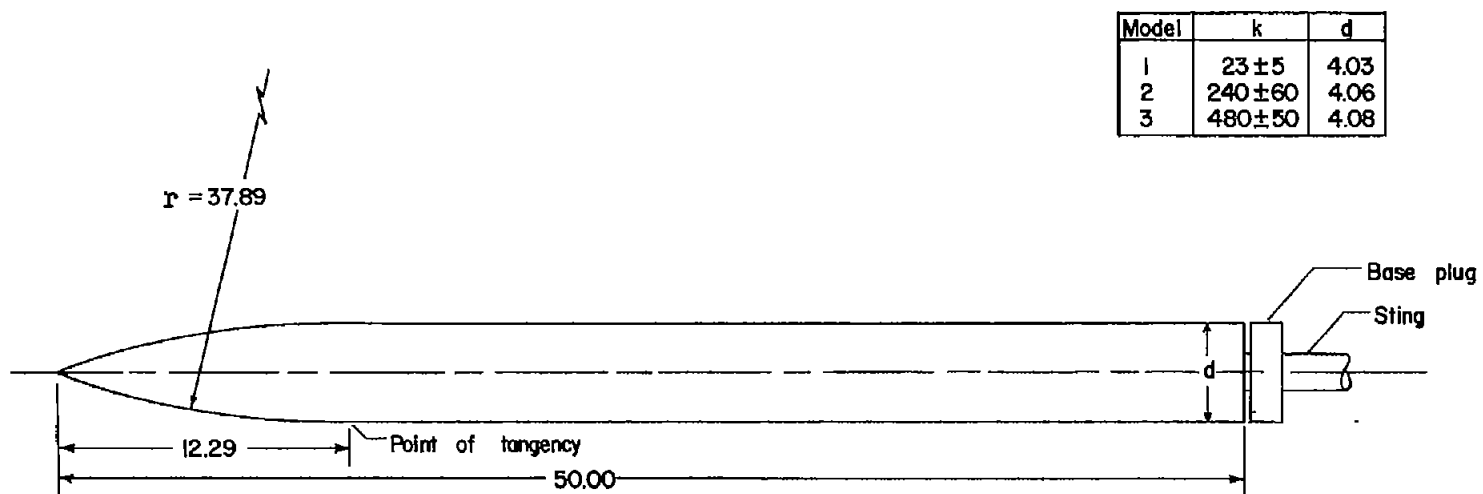
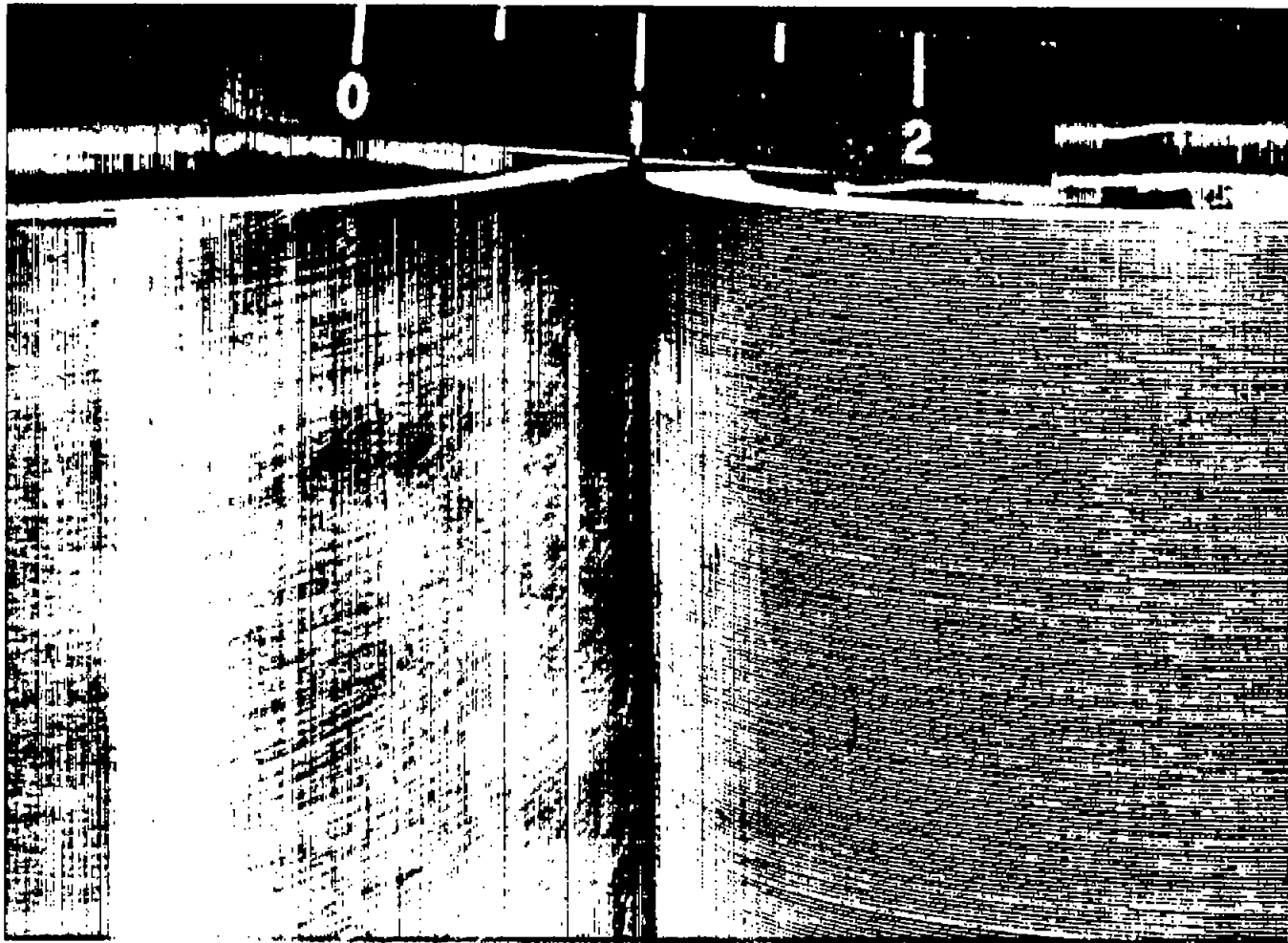


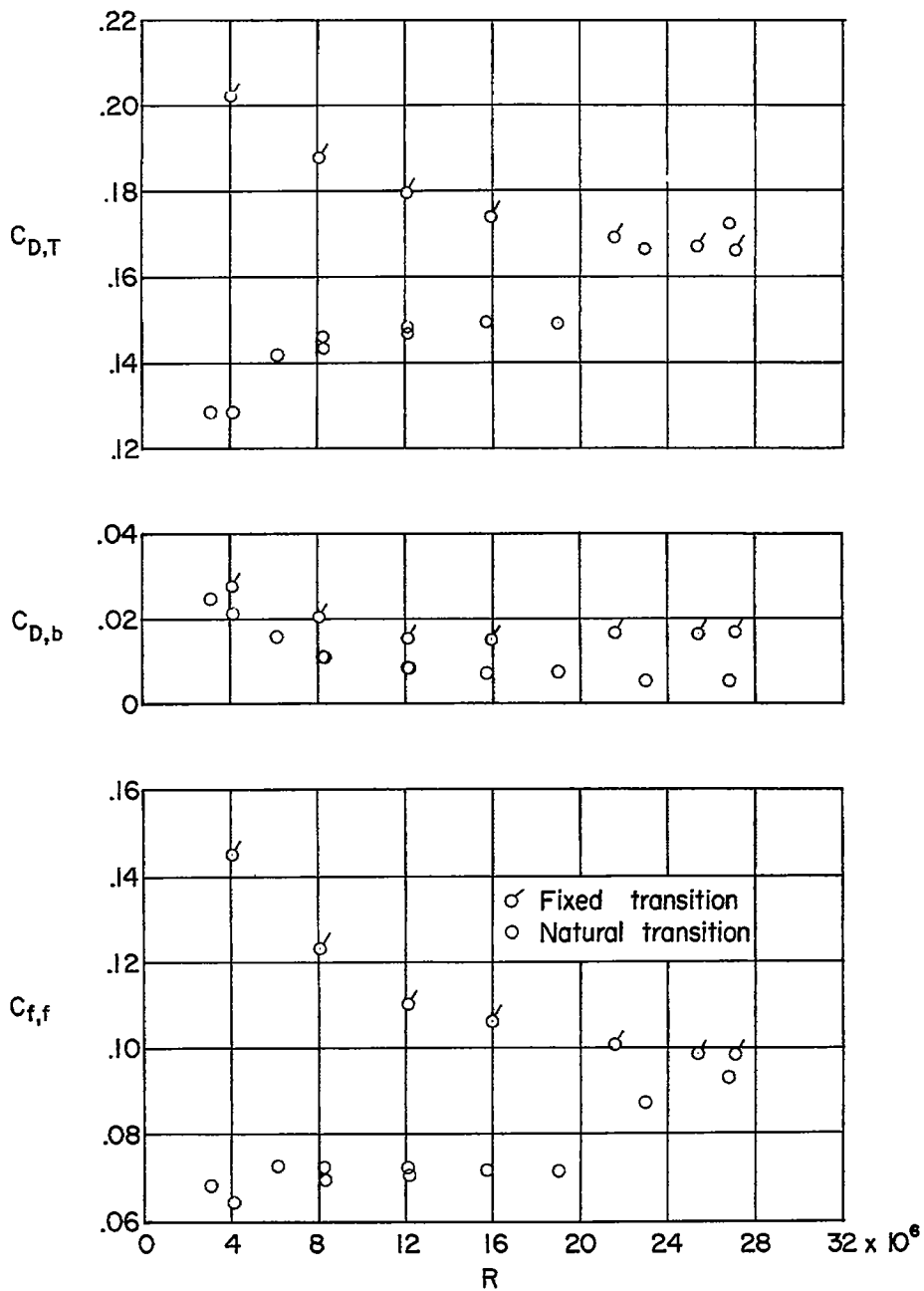
Figure 1.- Sketch of model. All dimensions are in inches except roughness height  $k$ , which is in microinches root mean square.



(a) 23-microinch model.

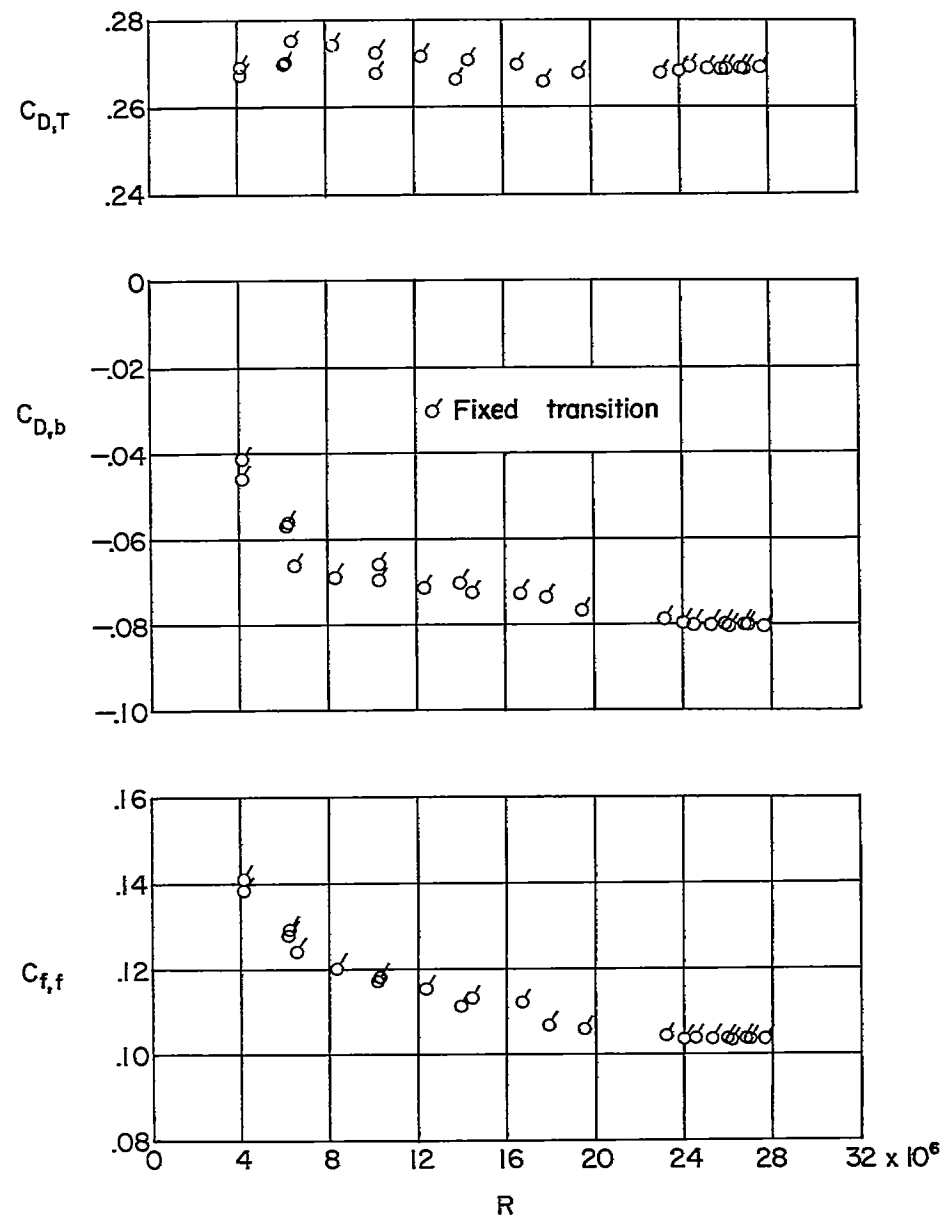
(b) 480-microinch model. L-82581

Figure 2.- Details of surfaces of 23- and 480-microinch-roughness models.



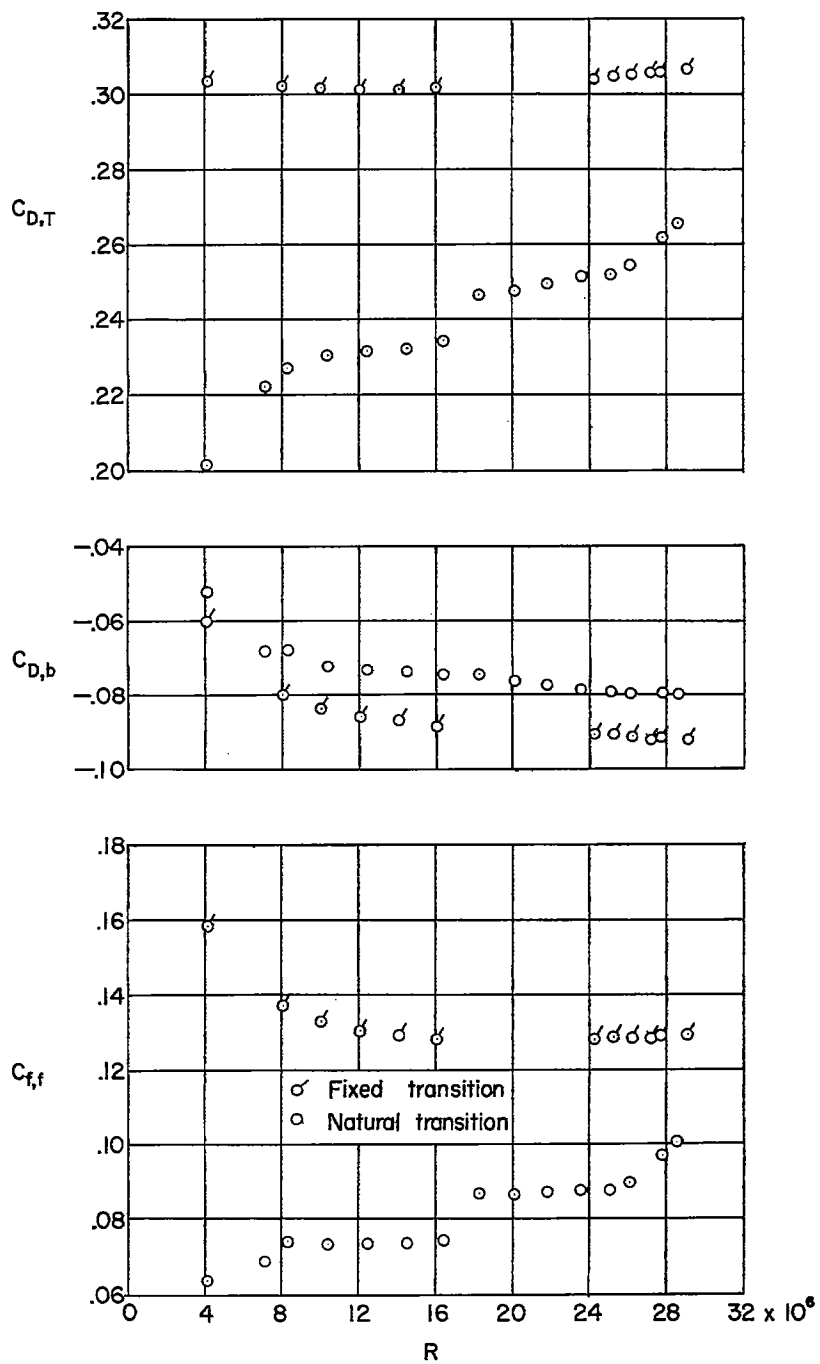
(a) 23-microinch-roughness model.

Figure 3.- Representative variation of  $C_{D,T}$ ,  $C_{D,b}$ , and  $C_{f,f}$  with Reynolds number for natural and fixed transition.



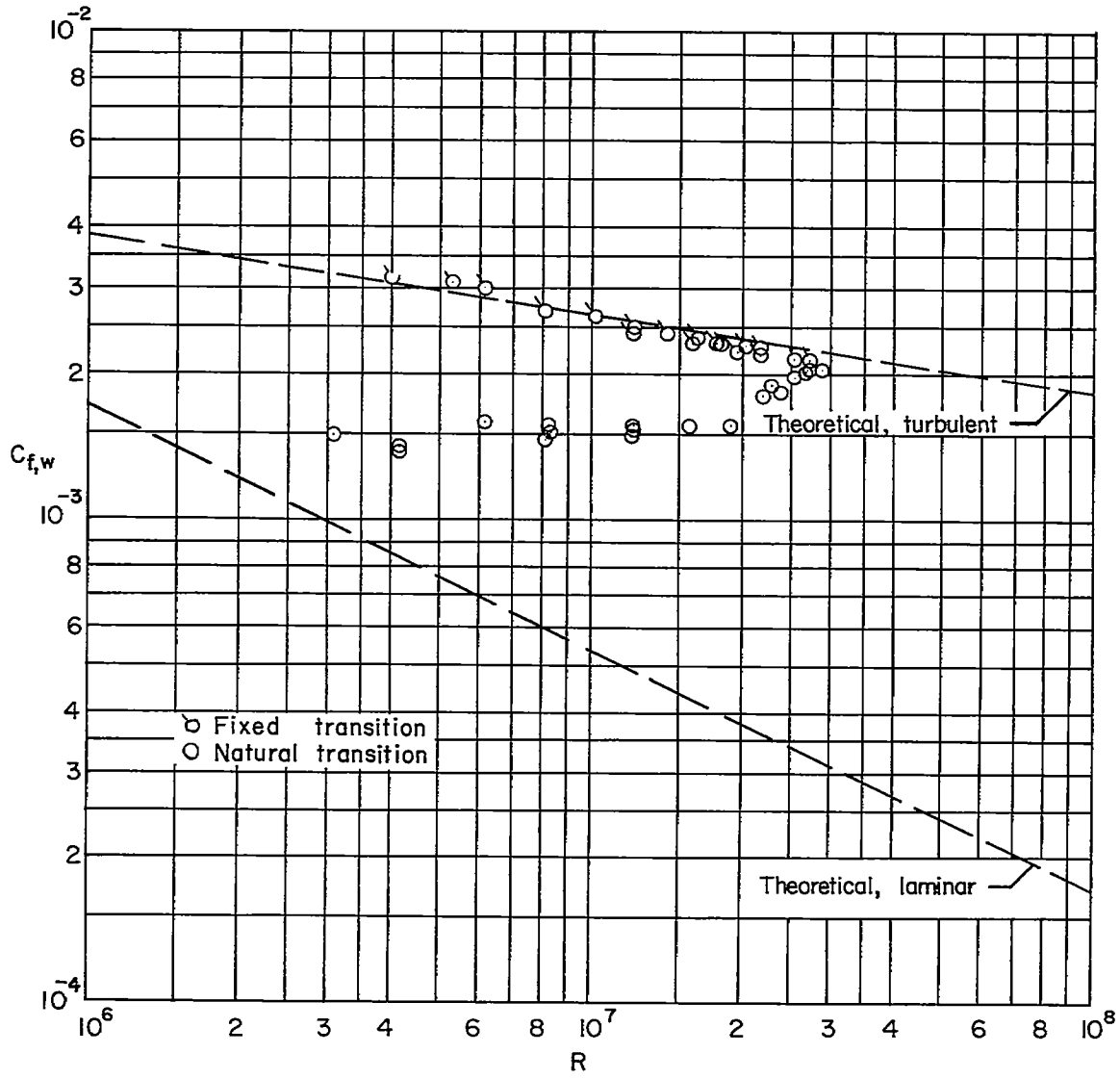
(b) 240-microinch-roughness model.

Figure 3.- Continued.



(c) 480-microinch-roughness model.

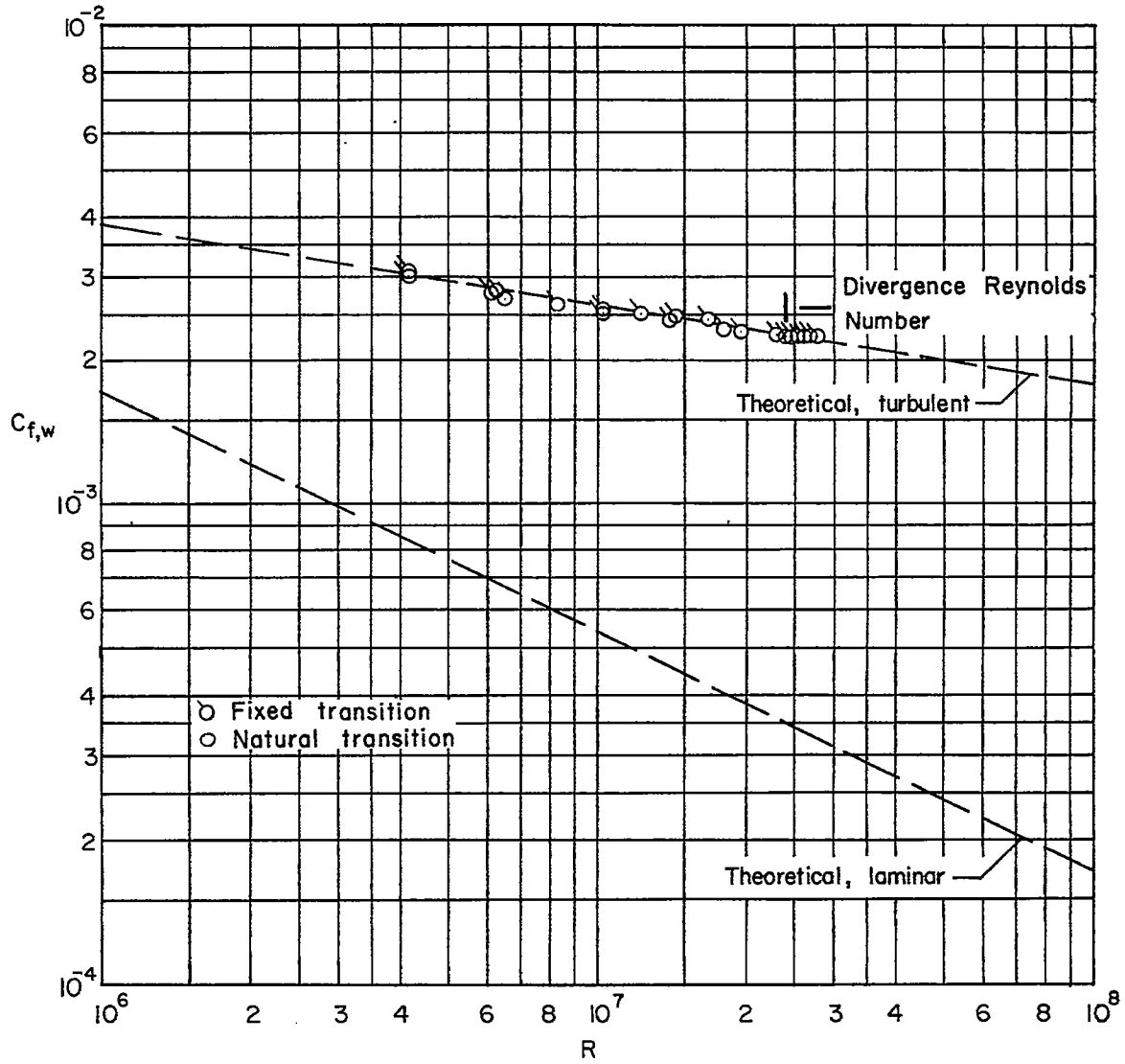
Figure 3.- Concluded.



(a) 23-microinch-roughness model.

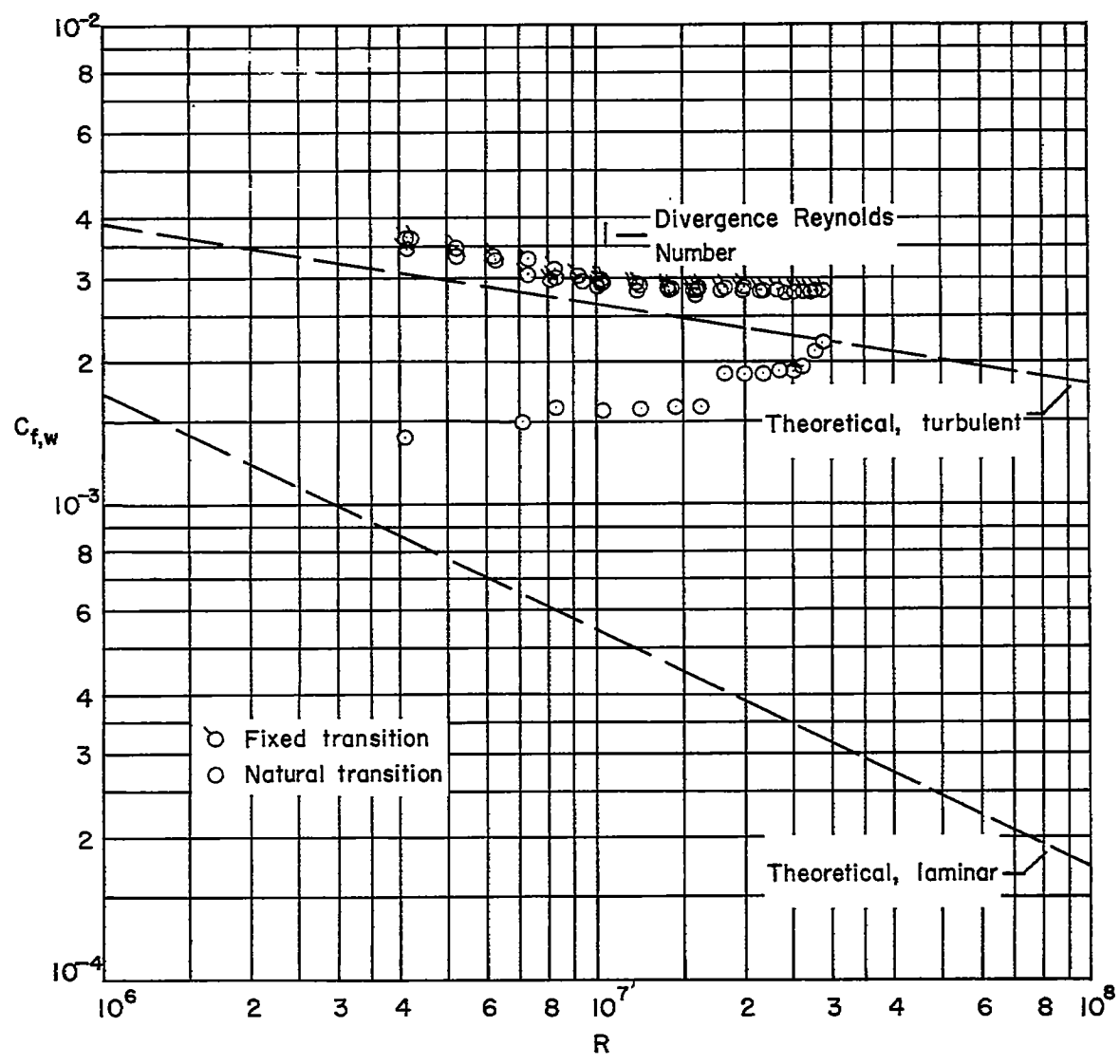
Figure 4.- Variation of skin-friction drag coefficient based on  $S_w$  with Reynolds number for several values of surface roughness.





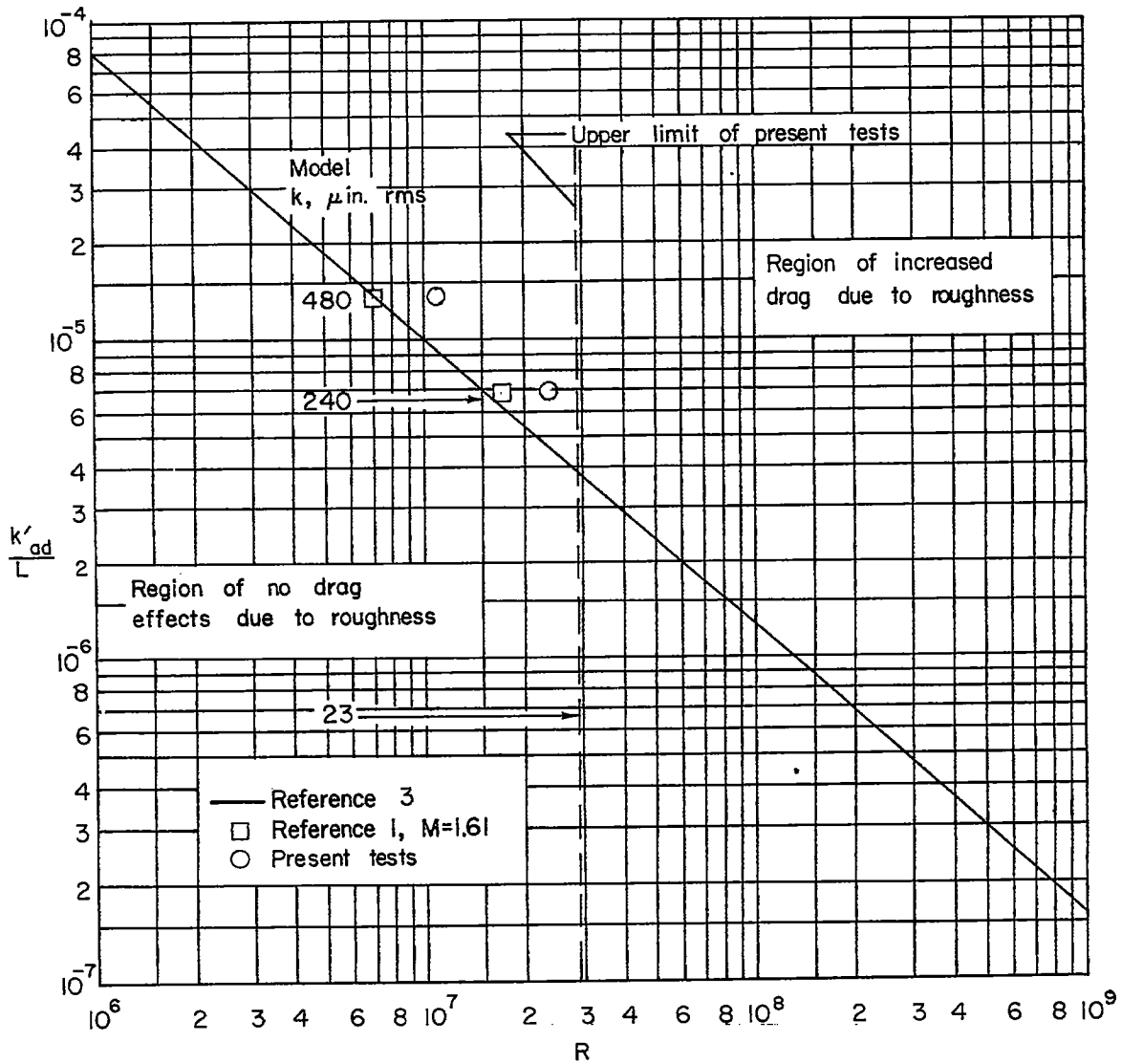
(b) 240-microinch-roughness model.

Figure 4.- Continued.



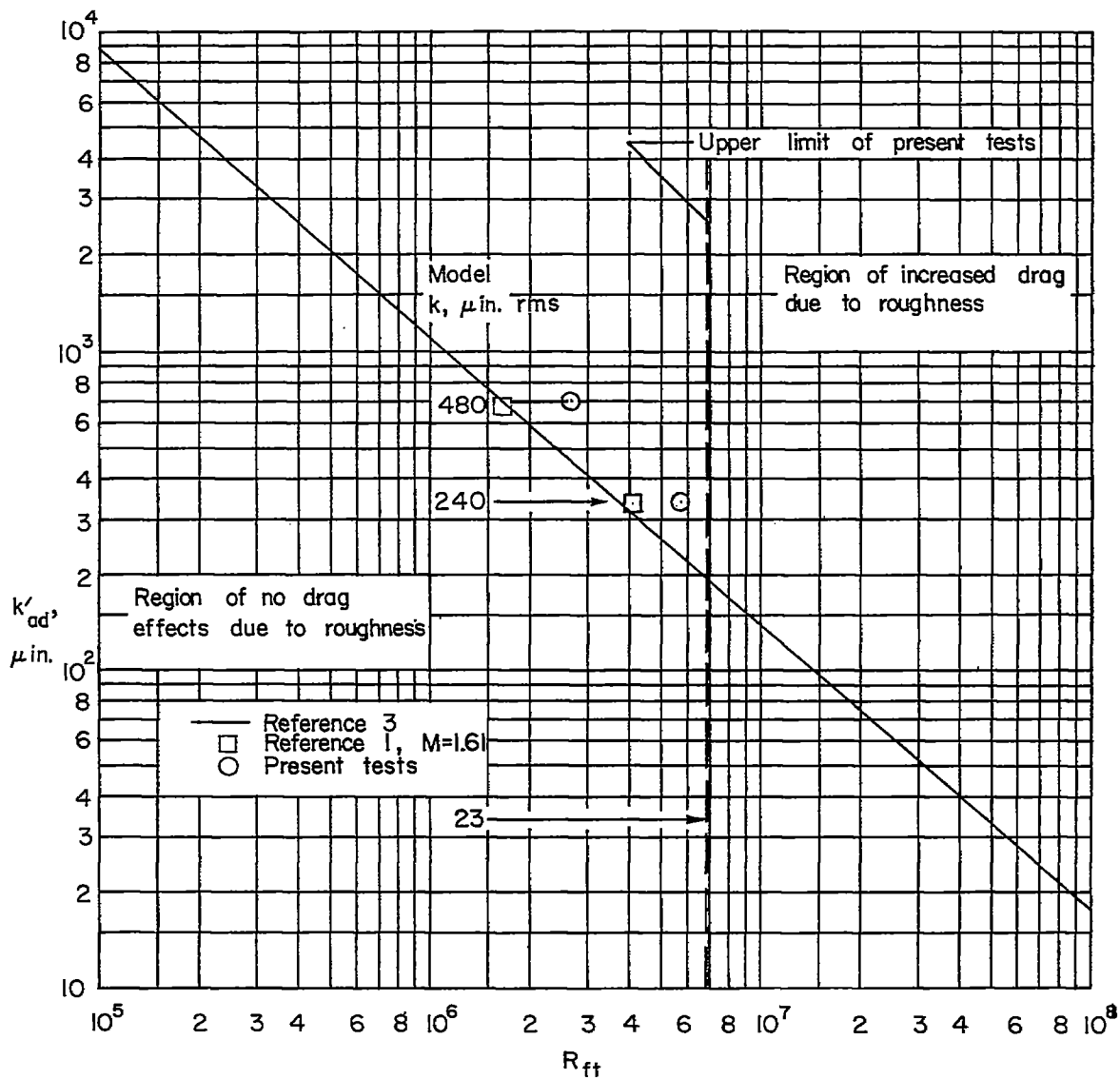
(c) 480-microinch-roughness model.

Figure 4.- Concluded.



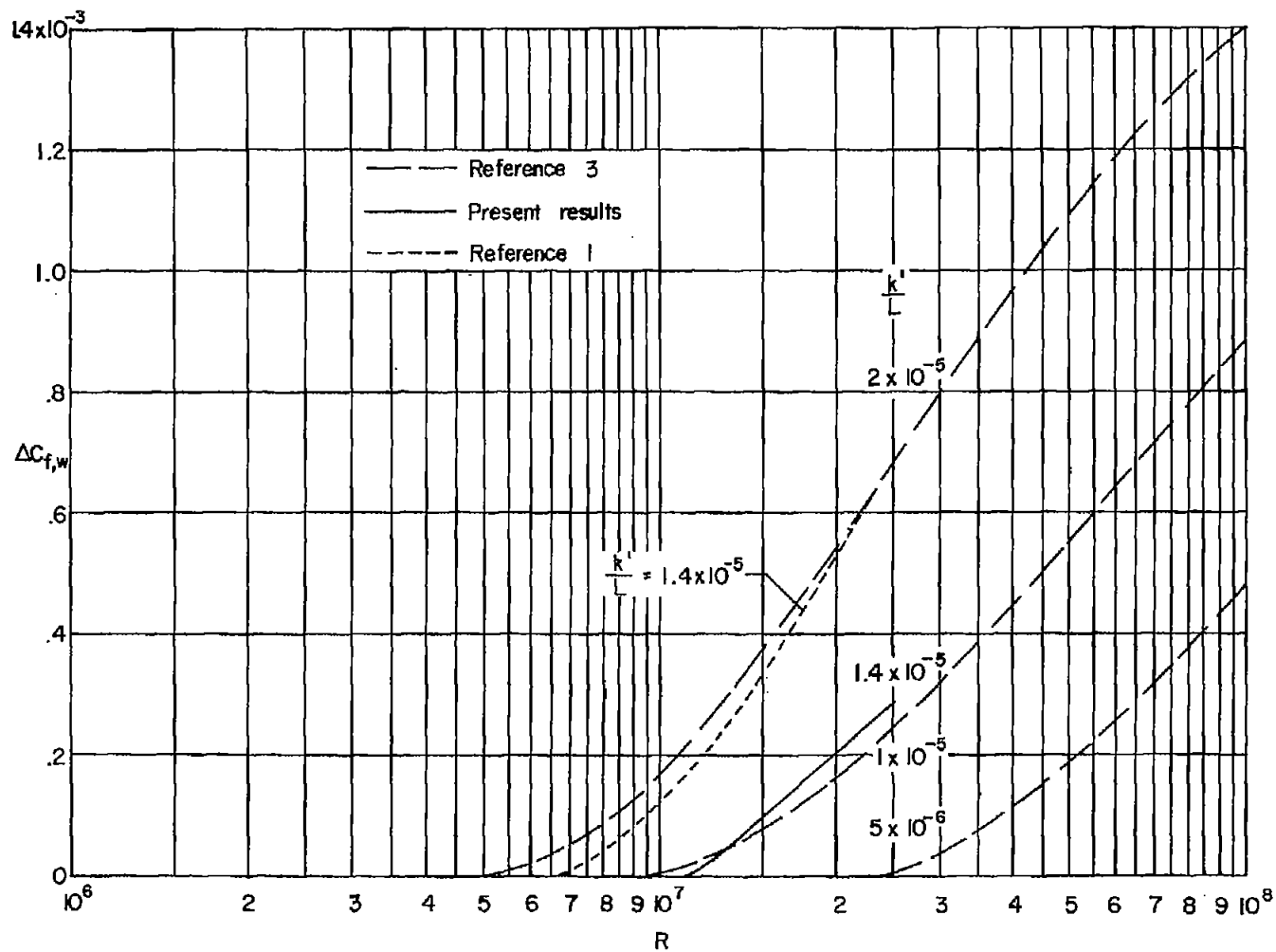
(a)  $k'_{ad} L$  as a function of Reynolds number.

Figure 5.- Comparison of allowable roughness results for ogive-cylinder at  $M = 1.61$  and  $M = 2.01$  and comparison with low-speed data for sand-roughened flat plate.



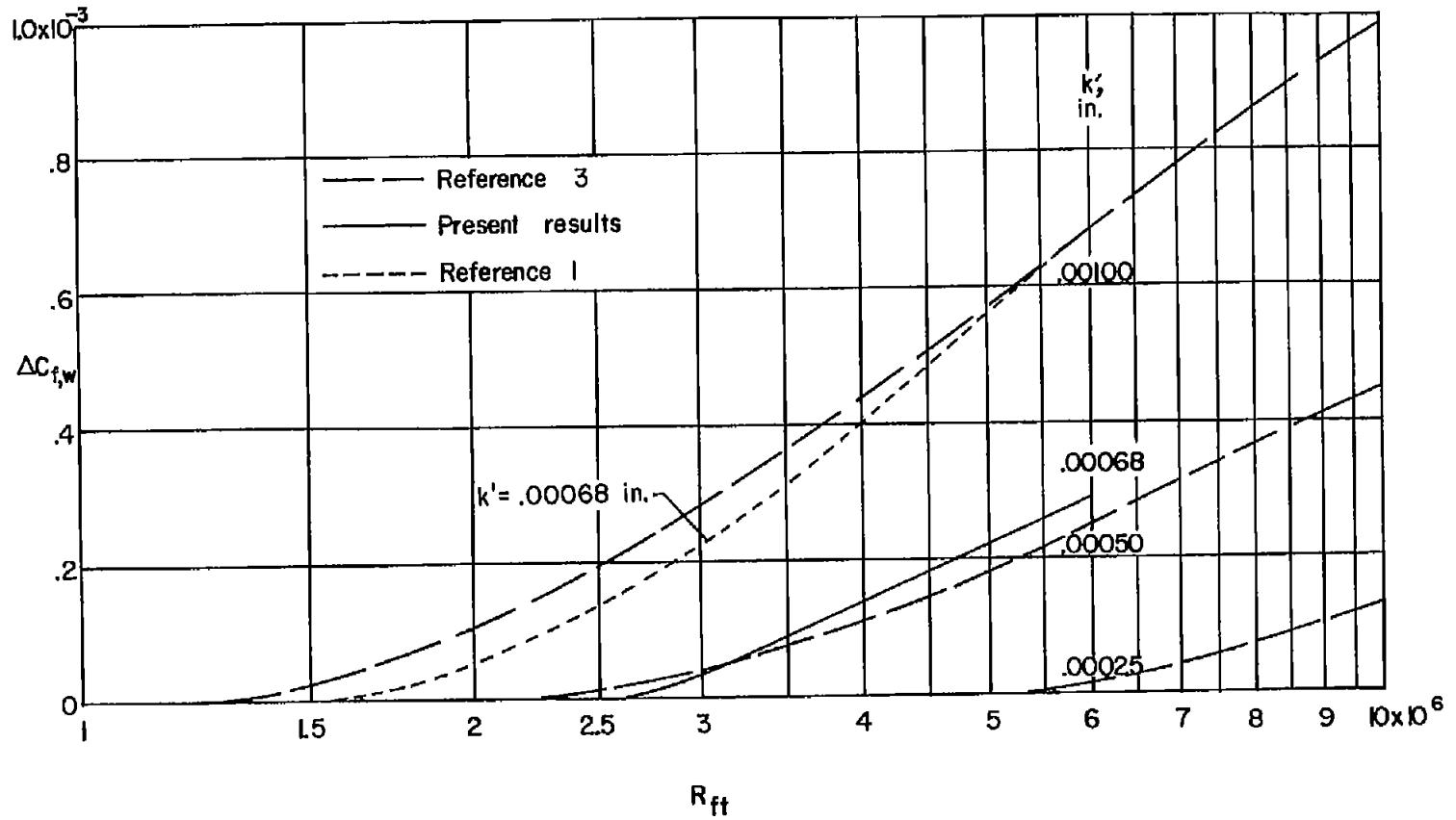
(b)  $k'_{ad}$  as a function of Reynolds number per foot.

Figure 5.- Concluded.



(a)  $\Delta C_{f,w}$  as a function of Reynolds number.

Figure 6.- Variation of  $\Delta C_{f,w}$  with Reynolds number for various values of  $k'$  and  $k'/L$ .



(b)  $\Delta C_{f,w}$  as a function of Reynolds number per foot.

Figure 6.- Concluded.



Figure 7.- Representative schlieren photograph of 480-microinch-roughness model. L-57-2758  
 $R_{ft} = 6.9 \times 10^6$ .

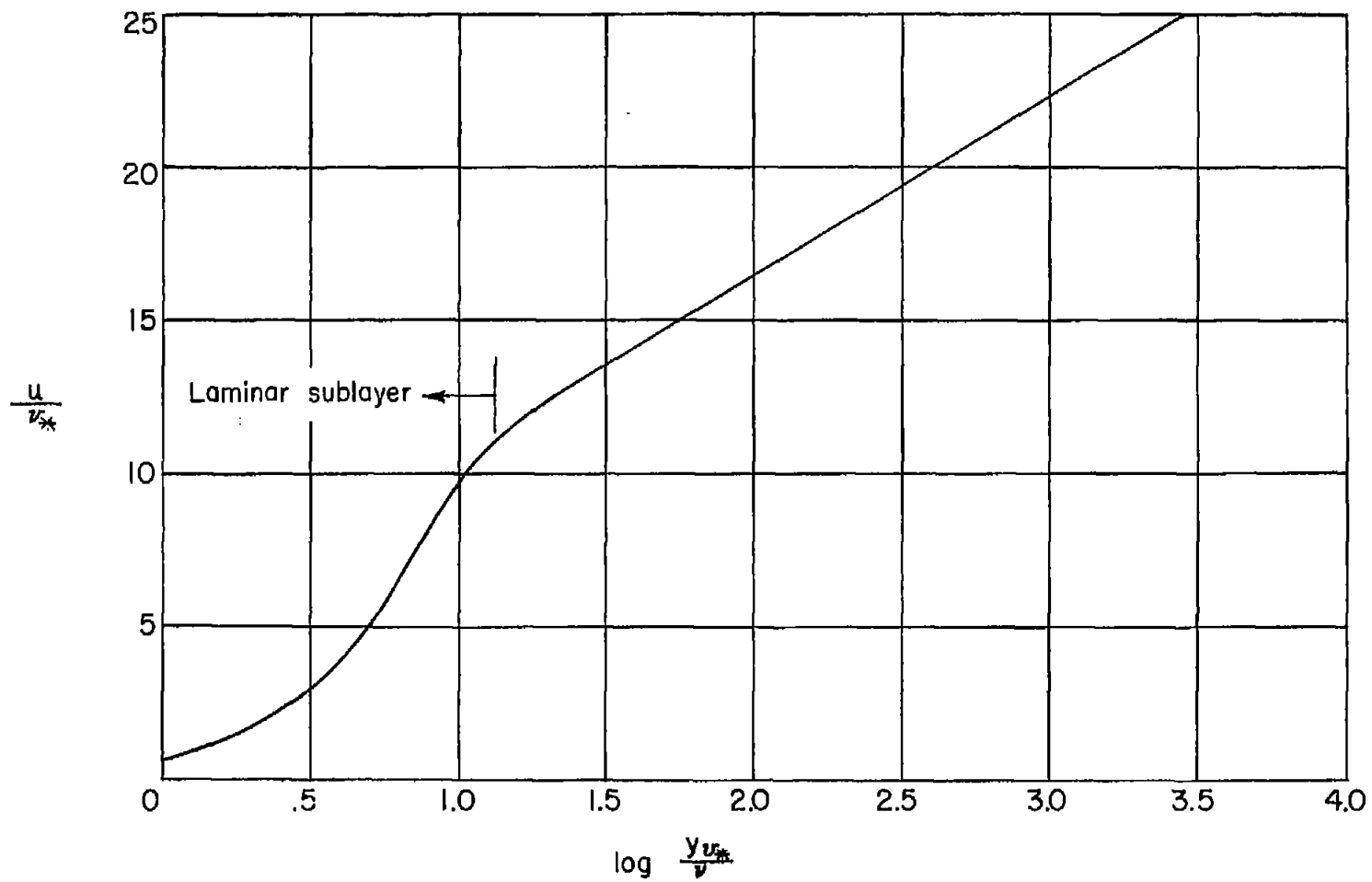


Figure 8.- Universal velocity distribution.